# Photosensitive Polymer from Ionic Self-Assembly of Azobenzene Dye and Poly(ionic liquid) and Its Alignment Characteristic toward Liquid Crystal Molecules

**Sufang Xiao, Xuemin Lu, and Qinghua Lu***

*School of Chemistry and Chemical Technology, Shanghai Jiao Tong University, Shanghai 200240, P.R. China*

*Received April 27, 2007; Revised Manuscript Received August 16, 2007*

ABSTRACT: A new strategy based on ionic self-assembly technology was provided for design of photosensitive material as liquid crystals (LC) alignment layer. The complex material was constructed by the coupling of poly(ionic liquid) and photosensitive unit azobenzene dye methyl orange. The structure, phase behavior and photoresponse were examined by a variety of techniques including FTIR, NMR, thermal analysis, polarized optical microscopy, X-ray diffraction, small-angle X-ray scattering, and birefringence measurements. Highly ordered lamellar nanostructure and photosensitive character were confirmed. Under the irradiation of pulsed UV laser with certain fluences, a pronounced optical anisotropic surface with the preferred direction perpendicular to the pulsed polarization or regular periodic grooves microstructure surface parallel to the pulsed polarization was obtained. The anisotropic surface of oriented molecular chain or topography was demonstrated to result in the alignment of LC by the optical transmittance plot and polarizing microscopy images of LC cells with different rotation angles.

## Introduction

The design of materials through noncovalent strategies, namely self-assembly or self-organization processes, including hydrogen bonding, coordination binding, acid−base interaction, and ionic self-assembly (ISA), is becoming one of the primary frontiers of materials research.[1−3] As a viable and facile route to design various functional or structured materials, ISA has been gaining increasing attention. ISA mainly employs electrostatic interactions to bind the oppositely charged tectonic units together, and the complex architectures can be tuned by the selection of constituents according to the desire of different applications. Recently, many fascinating results have been obtained in the ISA of multi- or monocharged rigid tectonic units and soft surfactants.[4−13] Ionic complexation of polyelectrolyte and oppositely charged low molecular mesogenic units or surfactant also has been exploited in many systems, aiming to produce liquid crystalline polymers with long-range order.[3,14−23]

Polymers containing azobenzene chromophores have attracted great interest in recent years due to their high optical sensitivity.[24,25] Under actinic irradiation, azo groups display *E*/*Z* isomerization and induce optical anisotropy, which have great potential applications in many fields such as information storage, optical memory and processing, waveguide switch, etc. Presently, various photosensitive materials have been exploited by doping low-molecular-weight azo dyes in polymers or covalent synthesis of azo polymers including side chain,[26,27] main chain,[28] and dendrimers.[29] However, doping films usually have low azo content due to poor compatibility, moreover the obtained photoinduction proved to be temporally unstable.[24,30] Photosensitive materials obtained from traditional chemical synthesis, compared with doped film, have better photoinduction stability; nevertheless, the synthetic processes usually were rigorous and fussy and involved many steps with low yield.[26−29] So the design of photosensitive polymers with optimizing properties to satisfy different applications is still the most attractive target.

Another interesting phenomenon that occurred on the light irradiation of azo−polymer is the generation of a periodic surface microstructure.[31,32] Generally, two methods can be employed to fabricate surface microstructure. One is the irradiation of two-beam interference of a continuous or nanosecond pulsed laser. The surface microstructure obtained by this method is called surface relief grating (SRG), which has been intensively studied in the past few decades.[33−36] The other way to fabricate surface microstructure is the irradiation of a single-beam nanosecond pulsed laser.[37−40] The interference of incident laser and laser scattered by the film surface results in the periodic surface microstructure, which is namely the laser-induced periodic surface structure (LIPSS). In comparison with SRG, LIPSS fabrication is more simple, and this structure was found to be very effective in aligning LC molecules.[41−43] Compared to the well-established mechanism for SRG, there are still some disputes on the mechanism of LIPSS formation; nevertheless, they may be attributed to the result of thermally induced macroscopic mass movement procedure of surface molecules. According to our previous studies, the formation of LIPSS is accompanied by the orientation of the molecular chain, which can be used to control the direction of the LC alignment.[32]

Here, we design a novel photosensitive supramolecular material by the ionic self-assembly of poly(ionic liquid) (PIL) and azobenzene dye with the aim to develop a new approach of creating functional materials for LC alignment and other applications. A commercially available methyl orange (MO) dye was selected as the building unit due to its capability for photoisomerization. The PIL was selected as a main chain segment for the following reasons: (I) it can be easily synthesized and designed by careful modulation of cationic structures and the selection of suitable anions; (II) PIL is environmentally friendly because the processes for its synthesis and employment only involve water and ethanol; (III) as a class of novel high-performance polyelectrolytes, it possesses high

---

* Corresponding author. E-mail address: qhlu@sjtu.edu.cn. Tel. & Fax: +86-21-54747535.

10.1021/ma070972s CCC: $37.00

**Scheme 1. Synthesis of PIL and the Complex of PIL and MO**

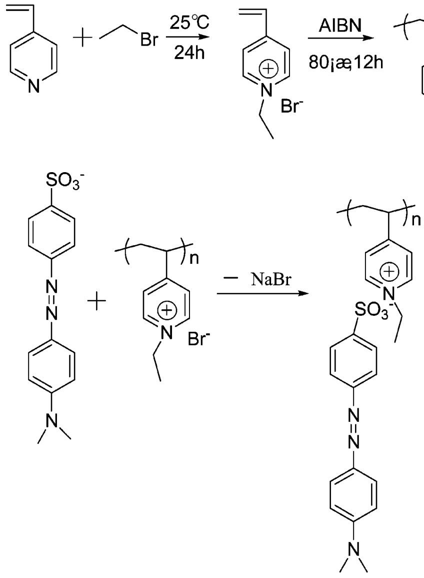

thermal stability and favorable properties of ionic self-assembly. Moreover, we believe that these preliminary studies may put more insight into the applications of the polymerized ionic liquid. In this paper, the complexed materials were studied by a variety of techniques including FTIR, NMR, polarized optical microscopy (POM), X-ray diffraction, small-angle X-ray scattering (SAXS), UV−vis spectra, birefringence measurements, and so on. Furthermore, we investigated the photoorientational properties of the obtained complex films by single−beam pulsed laser irradiation and evaluated the performance of the ISA polymer in noncontact LC alignment.

## Experimental Section

**Materials.** Methyl orange was purchased from the Sinopharm Chemical Reagent Company and used without further purification. The nematic liquid crystal 4-n-pentyl-4′-cyanbiphenyl (5CB) was obtained from Slichem LC Materials Company, Shijiazhuang, China. All reagents were of analytical grade. The water used was doubly distilled.

**Preparation of ISA Complexes.** Poly(1-ethylvinylpyridinium bromide) was prepared according to Scheme 1. $^1$H NMR (400 MHz, DMSO-$d_6$): $\delta$ 8.99 (2H, pyridine-H), 8.04(2H, pyridine-H adjacent to main chain), 4.57 (2H, $CH_2$), 1.54−0.51 (5H, $-CH_2-CH-$ and $CH_3$) as marked in Figure 2. The average molecular weight was about 12600 determined by gel permeation chromatography. For the preparation of ISA complex, 2 mg/mL PIL aqueous solution was added dropwise to MO aqueous solution with the same concentration, i.e., in a 1:1 molar charge ratio. The precipitated complex was centrifuged and washed five times with doubly distilled water to remove residual salts and possible noncomplexed precursors and then dried in a vacuum at 60 °C for 12 h.

The PILMO films were prepared by spin-coating a chloroform/ethanol (9/1) solution (30 mg/mL) onto quartz plates and glass slides (speed, 2000 rpm; time, 18 s). The thickness of the resultant film was about 100−130 nm indicated by atomic force microscopy (AFM).

**Instruments and Characterization.** Fourier transform IR (FTIR) spectra were recoded on a Perkin-Elmer Paragon1000 FTIR spectrometer on pressed thin transparent disks of the samples mixed with KBr. Spectra were obtained by collecting and averaging 64 scans. Nuclear magnetic resonance ($^1$H NMR) studies were carried out with a Varian Mercury Plus 400 MHz spectrometer in DMSO-$d_6$ solvent at room temperature (*ca.* 25 °C). The chemical shifts were referenced relative to tetramethylsilane. Wide-angle X-ray diffraction (WXRD) was performed on a Bruker-AXS D8 diffractometer (Cu Kα radiation $\lambda = 0.154$ nm, $U = 40$ kV, $I = 100$ mA). Differential scanning calorimetry (DSC) was performed on a Perkin-Elmer DSC-7 instrument with a 10 °C/min heating rate from −20 °C to 200 °C under nitrogen. Thermogravimetric analysis was performed using a Perkin-Elmer model 7 instrument. Samples were heated at 20 °C/min from room temperature to 600 °C in a flowing nitrogen atmosphere. Polarized optical microscopy was performed on a Leica DMLO microscope with a Leitz 350 hot stage. The surface morphologies of PILMO films were investigated by AFM (Digital Instruments Inc., Nanoscope IIIa) in contact mode. UV−vis spectra of the PILMO films were recorded using a Perkin−Elmer lamda 20 UV−vis spectrophotometer. The polarized UV−vis spectra were measured using the same device equipped with a Glan-Taylor prism. Small-angle X-ray scattering experiments were performed using a Bruker Nanostar SAXS instrument at 25 °C. The X-ray source, a 1.5 kW X-ray generator (Kristalloflexn760) equipped with a Cu tube was operated at 35 mA and 40 kV. The scattering intensities and patterns were detected by a two-dimensional position-sensitive detector (Bruker AXS) with 512 × 512 channels. The magnitude of scattering vector is given by $q = 4\pi(\sin\theta)/\lambda$. where $2\theta$ and $\lambda$ are the scattering angle and incident X-ray wavelength (1.542 Å). The distance from sample to detector was 27.1 cm, and the exposure time was 2 h for each sample.

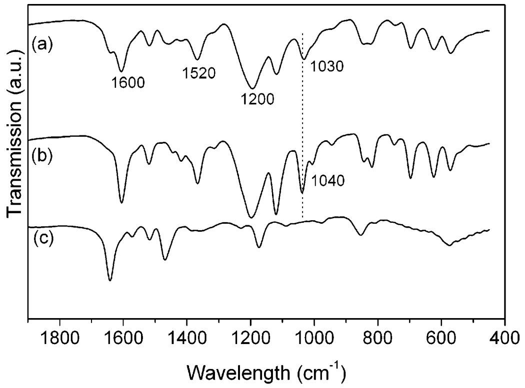

**Figure 1.** FTIR spectra of (a) PILMO, (b) MO, and (c) PIL.

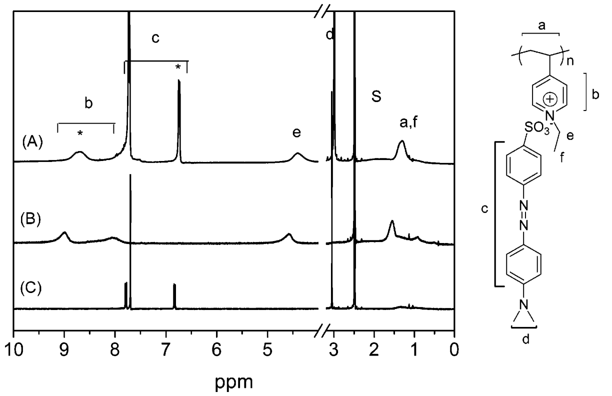

**Figure 2.** $^1$H NMR spectra of (A) PILMO, (B) PIL, and (C) MO.

Photoinduced birefringence measurements were investigated with a He−Ne laser at 650 nm as the probe light, which is far from the absorption band of the photochromic azo groups, and a continuous 532 nm laser as the pump light. The sample (spin-coating film with a thickness about 300 nm) was placed between two crossed polarizers in the path of 650 nm laser and was irradiated by the pump light linearly polarized at ±45° with respect to the vertical axis. The birefringence ($\Delta n$) value was calculated using:

$$I = I_0 \sin^2(\pi \Delta n d/\lambda)$$

where $I$ is the intensity of the transmittance, $I_0$ is the intensity of the probe beam, $\lambda$ is the wavelength, $d$ is the film thickness, and $\Delta n$ is the birefringence.

**Laser Irradiation and LC Cell Fabrication.** An *s*-polarized Nd:YAG laser (355 nm), with a pulse duration of 5 ns and repetition rate of 10 Hz, was used as light source. The polymer film was fixed on an $X-Y$ platform, and moving speeds were 0.1 and 5 mm/s in $X$ and $Y$ directions, respectively. The incident angle $\theta$ was fixed at 15° (Figure S1). A LC cell was fabricated by sandwiching nematic LC (5CB) between a PILMO-coated substrate and a counter buffing polyimide (PI) substrate. The two surfaces were separated by 10 $\mu$m spacers and held together using ethoxyline. 5CB was injected to the cell at its isotropic temperature by capillary action (Figure S2). Optical measurements were carried out by placing LC cells between crossed polarizers and measuring the transmittance from a He−Ne laser at 628 nm using a detector coupled to an oscillograph (Figure S3).

## Results and Discussion

**The Preparation and Characteristics of ISA Complexes.** The PIL was prepared according to Scheme 1. The obtained PIL polymer has excellent solubility in water. The ISA complex as precipitated was obtained by 1:1 charge ratio mixing of two aqueous solutions of MO and PIL as the Experimental Section described. The resultant complex does not dissolve in water, ethanol, THF, acetone, or nonpolar solvents and can only be dissolved in chloroform/ethanol (v:v 9/1), DMSO, and DMF. The successful formation of polymer complexes from poly(ionic liquid) and dye MO was demonstrated by the appearance of the FTIR band at 1600, 1520 cm$^{-1}$, corresponding to the characteristic peaks of phenyl bone stretching vibration, and at 1200, 1030 cm$^{-1}$, corresponding to the antisymmetric and symmetric stretching vibrations of the sulfonic groups(in Figure 1). Similar to the assembly of phosphate or alkylcarboxylic acid and polyelectrolyte,[15,19] we could observe the significant shifts from 1040 to 1030 cm$^{-1}$ in the symmetric stretching vibrations of the sulfonic groups due to binding.

The other impressive proof was provided by $^1$H NMR spectra of PILMO complexes and two building blocks in DMSO-$d_6$. As shown in Figure 2, all proton signals belonging to PILMO, PIL and MO are confirmed and marked clearly. The chemical shifts of 7.73 and 6.73 ppm in PILMO come from the proton signal of azo-moiety. In complex, the proton signals of azo-moiety undergo obviously broadening compared to the resolved resonances of small molecule MO due to its attachment to PIL. Moreover, the PIL motif signals of the complex have slight shift to upfield compared to the resource PIL, which result from the influence of the opposite negative charge unit. By comparison of the integral of the proton signal of PIL with that of MO labeled with asterisk, as shown in Figure 2, the ratio of integral areas is about 1:1, we can conclude that the stoichiometry of PILMO was about 1:1 (charge ratio).

Results from the UV−vis spectroscopic investigation of isolated MO, PIL and the resultant complexes PILMO in solution or film are presented in Figure 3. The UV−vis spectra of the materials are characterized by maxima in the range of 400 to 500 nm, which correspond to a strong $\pi-\pi^*$ transition of the E isomer of the azobenzene moiety.[4] The PIL has no absorbances in concerned range (curve b). Maxima of the absorbances of MO (solution in water) and the PILMO complexes in chloroform/ethanol (v:v 9/1)) are at 465 and 425 nm, respectively. The dramatic blue-shift of the maximum of the azobenzene chromophores in the complexes compared with pure dye implied the existence of aggregates, even at such low concentrations. This phenomenon can be ascribed to a strongly cooperative complex formation and aggregation process.[1,4,6] As shown in curve d, the maximum absorbances of the PILMO complexes in the film is 385 nm, which indicated that the aggregation is even more pronounced in the thin-film state.

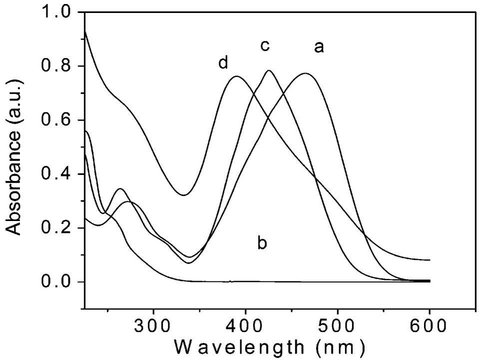

**Figure 3.** Normalized UV−vis spectra of (a) MO in water (*ca.* 10$^{-7}$ mol/L), (b) PIL in ethanol (*ca.* 10$^{-7}$ mol/L), (c) PILMO in chloroform/ethanol (v:v 9:1, *ca.* 10$^{-7}$ mol/L), and (d) PILMO film.

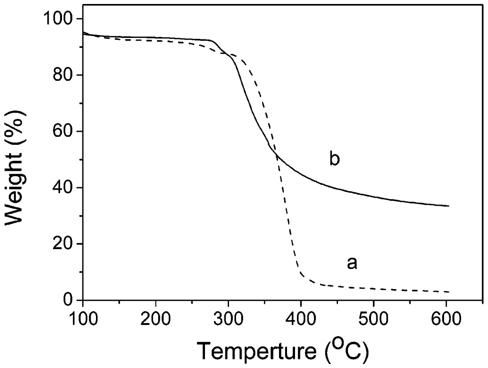

**Figure 4.** TGA curves obtained at a heating rate of 10 °C/min$^{-1}$ under a nitrogen atmosphere for (a) PIL and (b) PILMO.

The obtained powder material was subjected to thermal analysis to determine its stability. Thermogravimetric analysis shows the degradation of ISA complexes took place in one step except the 5% weight loss of $H_2O$ at about 100 °C, which illuminated that the PILMO was a kind of new and pure compound. The complexes are stable up to at least 275 °C, though it was slightly lower than that of the resource PIL due to the introduction of MO. Differential scanning calorimetry (DSC) was further performed to investigate the thermal behavior of this material. However, the curve did not show any structural thermal transitions in the range −20 to +220 °C. POM with hot stage was also performed and showed that the complexes melt to some extent when above 235 °C, but at the same time the samples started to blacken. Therefore, it is difficult to observe the characteristic texture by the direct melting of the obtained powder. The reason for this might be due to its rigid molecular structure[6,44] due to the absence of sufficient soft segments (without the presence of an alkyl spacer between the PIL main chain and rigid azobenzene). However, by casting from chloroform/ethanol (9:1) solution with a concentration of about 30 mg/mL, pronounced Schlieren textures could be observed in the POM (see Figure 5a), which indicated high orientational order of the complexes. It was found that the PILMO complex formed lyotropic phases in DMSO (approximately 30 wt %) as determined by POM (Figure 5b). The optical texture was similar to that of the cast film.

In order to put more insight into the phase present in the material, WXRD and SAXS measurements were performed for the complexes. WXRD analysis (Figure 5c) shows a broad peak at wide angle 20.1° and a sharp peak at small angle 3.3°. The wide-angle peak reflection at 20.1° suggested that no crystal exists in the complexes, which is consistent with the intrinsic character of mesophases.[45,46] The latter, at $2\theta = 3.3°$, is a first-order diffraction and indicates a lamellar structure with a thickness of 2.7 nm, which shows that the complex is organized in order at the side-chain scale. More convincing evidence for

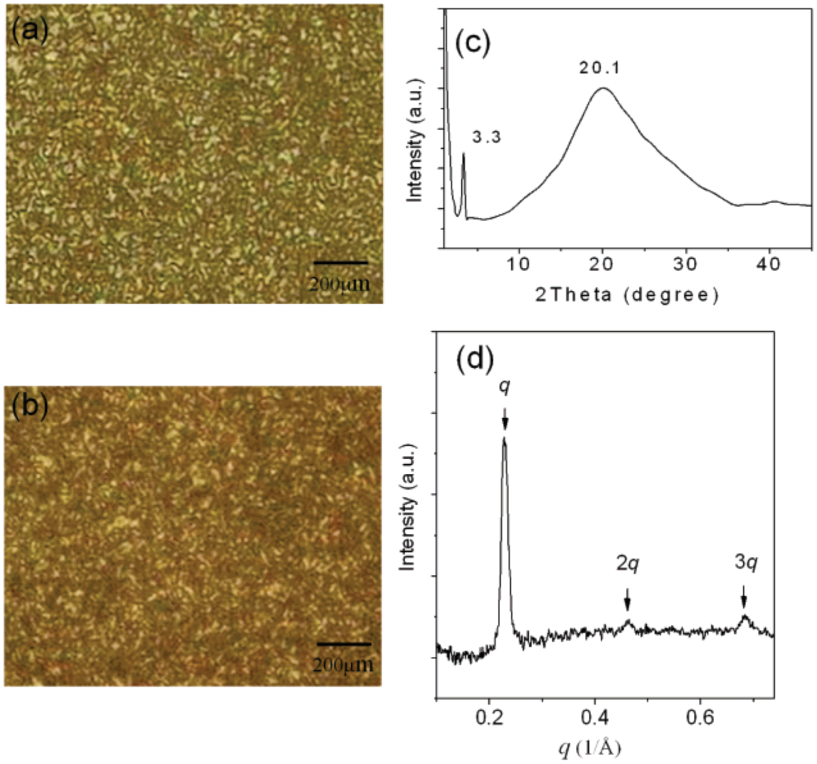

**Figure 5.** Characteristic texture of PILMO (a) film cast from chloroform, (b) DMSO solution (ca. 30% wt %) as observed in a polarized optical microscope. (c) WAXD and (d) SAXS patterns of PILMO at room temperature.

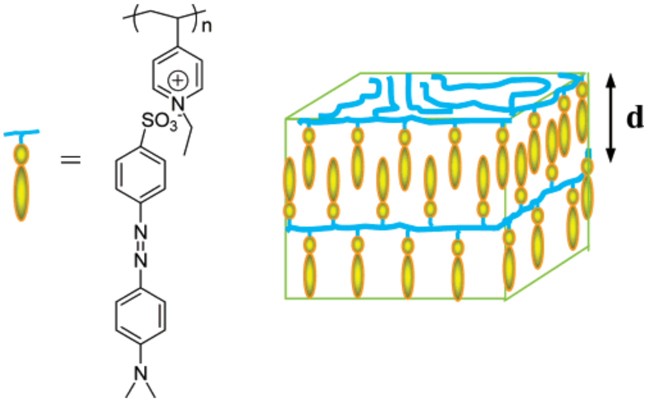

**Figure 6.** Schematic representation of the layered architecture obtained from PILMO complexes.

the lamellar nanostructure was provided by the SAXS result. As depicted in Figure 5d, the PILMO shows a clear scattering peak at $q = 0.23$ Å$^{-1}$ along with well-defined $2q$ (0.46 Å$^{-1}$) and $3q$ (0.69 Å$^{-1}$), which further verified the lamellar organization[47] with a periodicity of 2.7 nm. The SAXS result is in good agreement with WXRD analysis, and thus the lamellar nanostructure of the PILMO complexes was confirmed. On the basis of X-ray data and molecular calculations on the size of the side chain, we proposed the molecular organization model sketched in Figure 6 for the resultant supramolecular polymer. Within the PILMO lamellae, there exists lamellar self-assembly at a periodicity of 2.7 nm with alternating disordered PIL soft segments and the stacking of the MO rigid side-chain.

**Photoresponsive Character of the PILMO Film.** In order to explore the dynamic process of photoresponse and orientation in the complex film, birefringence measurements were performed. Here, the photoinduced $\Delta n$ upon irradiation with linearly polarized 532 nm light was probed by 650 nm weak probe light at 25 °C. The birefringence evolution with time is shown in Figure 7. The birefringence increased rapidly with the irradiation time increase at first, then relatively slowed down, and at last reached a saturation value after irradiation for about 300 s. For the present case, a steady value of $\Delta n$ to be about 0.067 was obtained under the irradiation of pump light with an intensity of 150 mW/cm$^2$. This birefringence behavior indicated that the PILMO was an ideal photosensitive material. Another noteworthy phenomenon was that the photoinduced birefringences showed a slight decay and then achieved a steady value ($\Delta n$, 0.060) after the pump light was turned off. The ultimate stable orientation was attributed to the rigid molecular structure and the fact that the orientation was stored in the aggregated phase.[48]

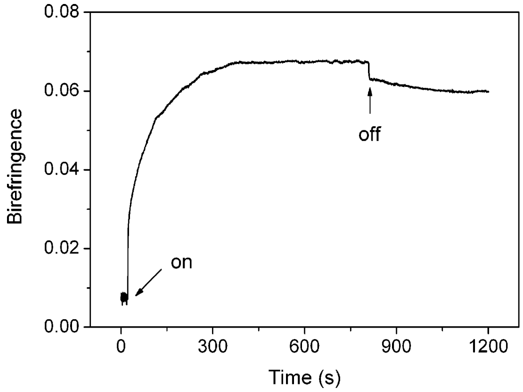

**Figure 7.** Evolution of the birefringence with time in PILMO film under irradiation with 532 nm linearly polarized light at room temperature. The moments of switching on and off of the pumping light are marked with arrows.

**LC Alignment on Irradiated PILMO.** In order to prove the potential uses of this novel liquid-crystalline material in devices or optical components, preliminary optical investigations in the field of LC alignment were performed. It is well-known that the alignment of LC molecules can be controlled by the

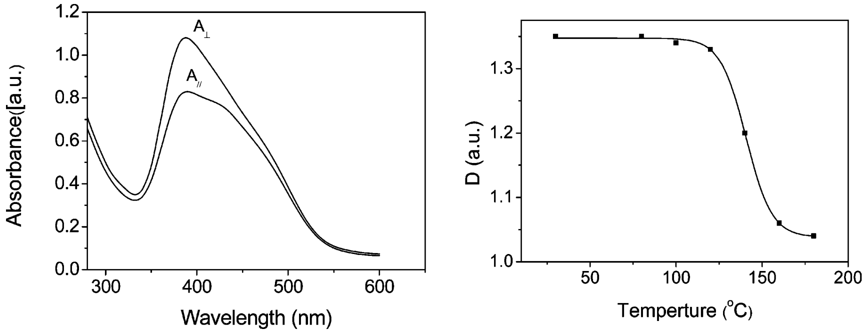

**Figure 8.** (a) Changes of polarized absorbance spectra in a film of the PILMO polymer under irradiation with pulsed UV laser at laser fluence of 3.6 mJ/cm$^2$. (b) Changes of the dichroism with temperature, the orientated films were annealed for 30 min at each temperature. $A_{||}$ and $A_\perp$ are the absorbance parallel and perpendicular to laser polarization direction (**E**), respectively. $D = A_\perp/A_{||}$.

anisotropic surface of the alignment layer, either by its topography or by an oriented molecular chain, which was referred to as the "command surfaces". Here, we investigated the photoinduced behavior of the ISA supramolecular complex film under irradiation of a pulsed UV laser to evaluate the validity for LC alignment.

In this work, an *s*-polarized laser (355 nm) was used as the light source. Different from the cast film, the spin-coated PILMO films were proved to be isotropic and uniform with low surface roughness by optical microscopy and AFM. First, we investigated the anisotropic orientation of azo groups in the complex film under laser irradiation with a fluence lower than the threshold of the formation of LIPSS. As shown in Figure 8a, a small irradiation dose of 3.6 mJ/cm$^2$ induced very pronounced anisotropic orientation. The absorbance in the direction parallel to the polarization of the laser beam is obviously smaller than that in the direction perpendicular to the polarization of the laser beam, which suggests that the preferred direction of the azobenzene chromophores is perpendicular to the laser polarization direction. For the practical application, the time and temperature stability of the orientated anisotropic surface is particularly important. Although the obtained dichroism was moderate, as presented in birefringence evolution plot, it achieved an ultimate stable value after irradiation was ceased. Here, the orientation stability was further tested in the large time scale by testing the changes of dichroism with time. After keeping the orientated film at room temperature for 2 months, negligible decrease of the dichroism was observed. The temperature stability of dichroism was testified by annealing the orientated films at 80−180 °C for 30 min. As shown in Figure 8b, the induced anisotropy is stable up to 120 °C.

To investigate the LC alignment on the azo-containing complexes after being irradiated by laser, a LC cell was assembled using the irradiated film of PILMO and a PI counter substrate buffed in the direction perpendicular to laser polarization acting on PILMO, isotropic 5CB was injected into the cell by capillary force and the cell gap was fixed to 10 $\mu$m using a polyethylene film. The cell was examined by placing LC cell between two crossed polarizers and measuring the transmittance from a He−Ne laser at 628 nm using a detector coupled to an oscillograph as shown in Figure S3. For a cell with uniform LC alignment between crossed polarizers, the transmittance changes with the rotation of LC cell with respect to the normal line of the substrate can be calculated according to the following formula:[32]

$$T = \sin^2(2\theta)\sin^2(\pi\Delta nd/\lambda)$$

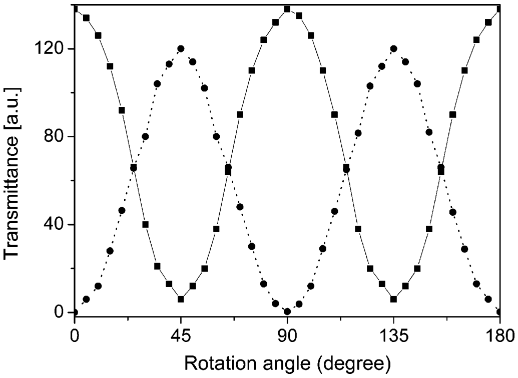

**Figure 9.** Optical transmittance of LC cells as a function of the rotation angle of the cell between crossed polarizers. The cell was assembled by a PILMO substrates irradiated with pulsed laser at a fluence of 3.6 (●) and 6.0 mJ/cm$^2$ (■) and a counter buffing polyimide substrate.

where $T$ is the transmittance of the light though the LC cell, $\theta$ is the rotation angle of the LC cell, $d$ is the thickness of the cell, $\Delta n$ is the refractive index of the filled LC molecules, and $\lambda$ is the wavelength of the detected laser. For a given cell, the terms except $\theta$ are fixed and the transmittance is only related to the rotation angle $\theta$. In our experiment, the initial position of LC cell was considered to be 0° when the buffing direction of the reference substrate was parallel to either polarization direction of the polarizers. In the case of 3.6 mJ/cm$^2$, as shown in Figure 9 (−●−), the LC cell exhibited a dark field at the initial position, indicating that the directions of LC alignment on the two substrates were parallel to each other, which suggests that the director of the LC molecules aligned parallel to the aligned chromophores in the film of the complexes. Optical transmittance of LC cells presents regular change according to the rotation angle of the cell between crossed polarizers, which confirmed that uniform alignment of the LC in parallel-mode was obtained in the combined LC cell. In addition, as shown in Figure 10, the POM images of LC cell with different rotation angles also further illuminated explicitly the alignment of LC. The light field presented alternative change of dark or bright under crossed polarizers according to the rotation of the cell with a period 90°, which further demonstrated that the homogeneous and stable LC alignment was achieved on the PILMO azo anisotropic orientation film. The scheme of the LC alignment in the cell was proposed in Figure 10c. Moreover, the photoorientation were performed using an ultrahigh-pressure Hg lamp equipped with Glan-Taylor polarizing prism and very effective induction of optical anisotropy was also observed. All these examples confirmed that the complexes are capable of light-induced anisotropy and can be used in the alignment of LC.

Laser-induced periodic structures on surface can be formed when the polymer is subject to enough pulsed laser fluence. For PILMO film, under the illumination of pulse UV laser, the

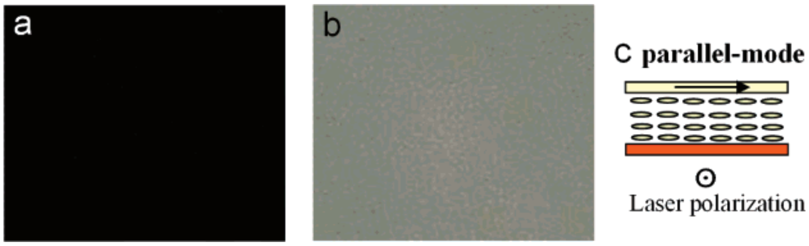

**Figure 10.** POM images of LC cell with alternative change of light field under crossed polarizers: (a) 0° /90°/180°/270°; (b) 45°/135°/225°/315°. (c) Scheme showing the LC alignment in the cell. The arrow indicates the buffing direction of the counter polyimide substrate. The cell was assembled with an irradiated PILMO substrate at a fluence of 3.6 mJ/cm$^2$ and a counter buffing PI substrate.

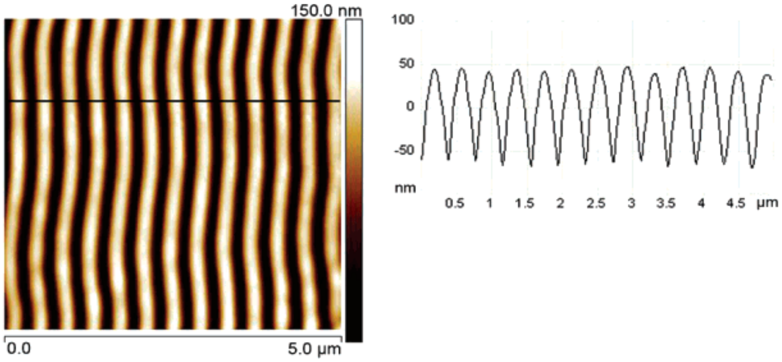

**Figure 11.** Typical AFM image of LIPSS on the PILMO film irradiated with pulsed UV laser at a fluence of 6.0 mJ/cm$^2$. Right: a cross-sectional profile along the line marked in the topographical image.

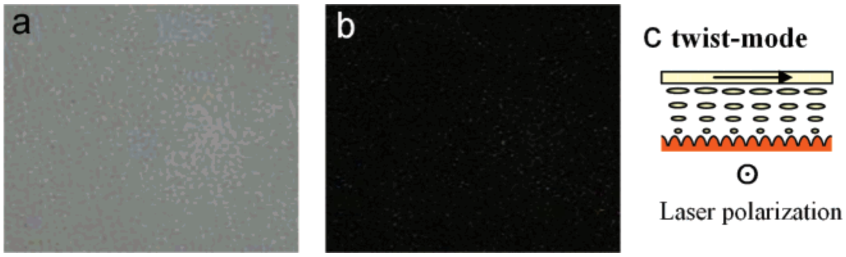

**Figure 12.** POM images of LC cell with alternative change of light field under crossed polarizers: (a) 0°/90°/180°/270°; (b) 45°/135°/225°/315°. (c) Scheme showing the LC alignment in the cell. The arrow indicates the buffing direction of the counter polyimide substrate. The cell was assembled with an irradiated PILMO substrate at a fluence of 6.0 mJ/cm$^2$ and a counter buffing PI substrate.

generation of LIPSS showed threshold behavior: no periodic microstructure was formed until the fluence reaches a critical value 3.8 mJ/cm$^2$. The experiment results demonstrated that LIPSS amplitude increased markedly with laser fluences followed by leveling off at a fluence of 5.6 mJ/cm$^2$, and then decreased when the laser fluence higher than 9.0 mJ/cm$^2$. The phenomenon was consistent with that of covalent polymer, which was attributed to the mechanism of LIPSS formation being considered to be a result of thermal induced macroscopic mass movement procedure of surface molecules.[42,49] As shown in Figure 11, rather regular periodic grooves microstructure was obtained on the PILMO films after irradiation at a fluence of 6.0 mJ/cm$^2$. The cross-sectional profile of the grooved structure indicated nearly sinusoidal variation of the groove shape with 100−110 nm depth. The period of the grooved structure depends strongly on the incident angle of the laser beam. In our case, the period was typically 396 nm for a 15° incident angle. Moreover, the annealing experiments proved that the LIPSS film has high thermal stability with an erase temperature of 130 °C.

To investigate the behavior of LC alignment on the PILMO with periodic grooves, a LC cell was also fabricated with the laser-irradiated PILMO substrate (with laser fluence of 6.0 mJ/cm$^2$) and a buffing PI substrate with the buffing direction on the PI substrate perpendicular to the laser electric vector **E** for the irradiated PILMO film. The transmittance of He−Ne laser through LC cells was present in Figure 9 (−■−). The dependence of optical transmittance on the rotation angle of LC cell between crossed polarizers with a period of 90° demonstrated that homogeneous LC alignment was achieved on the PILMO films. In the case of 6.0 mJ/cm$^2$, the LC cell exhibits maximum transmittance at the initial position, indicating that the direction of LC alignment on the two substrates were perpendicular to each other (twist-mode LC cell); i.e., the LC molecules on the laser-irradiated PILMO film were controlled by topography and aligned along the microgrooves of LIPSS. As shown in Figure 12, the alternative change of light field with a period of 90° further illuminated explicitly that a homogeneous and stable LC alignment was achieved on the LIPSS orientation film. The scheme of the LC alignment in the cell was proposed in Figure 12c. Thus, the photosensitive ISA material can provide two approaches with different alignment modes to control LC direction just by adjusting the irradiated laser fluence, and we believe it has great potential in mutidomain LC display and other optical designs. Related systemic studies will be explored.

## Conclusions

In this contribution, we designed a novel photosensitive supramolecular material by the ionic self-assembly of poly(ionic liquid) and azobenzene dye methyl orange. A highly ordered lamellar nanostructure with a periodicity of 2.7 nm was identified by means of X-ray diffraction and SAXS measurements. The birefringence measurements proved that the complex films possess fast optical response and a strong photoinduced anisotropy with excellent stability. The resultant ISA material in noncontact alignment of liquid crystal was further exploited. Under pulsed UV laser irradiation with fluence lower than the threshold of LIPSS, for example of 3.6 mJ/cm$^2$, a pronounced optical anisotropic surface with the preferred direction perpendicular to the pulsed polarization was obtained and successfully tested for the alignment of LC. Under the illumination of pulsed UV laser at fluences from 5.6 to 9.0 mJ/cm$^2$, a regular periodic grooves microstructure was obtained with high thermal stability. Uniform alignment of the LC with a twist of 90° was obtained in a combined LC cell made up of a PILMO coated substrate with LIPSS and a buffed polyimide. The optical transmittance plot and POM proved that LC aligned along the microgrooves of the PILMO surface. All the results demonstrated that the obtained ionic-bonding polymer can be used as a photosensitive material in many potential fields. This offers a new possibility for the design of complexed functional materials, which are not easy to synthesize by traditional chemical approaches. In addition, for PIL, a new application view of the construction of functional materials was exploited, excepting the well-known fields of new solar cells, lithium batteries, supercapacitors, sensing materials, and so on.

**Acknowledgment.** We gratefully acknowledge the support of the National Science Foundation of China (Grant No. 60577049) and projects (05JC14019, 0652nm017) of the Science and Technology Commission of Shanghai Municipal Government.

**Supporting Information Available:** Figures showing the optical setup for laser irradiation, scheme of fabrication of liquid crystal cell, and setup for optical transmittance measurements of liquid crystal cells. This material is available free of charge via the Internet at http://pubs.acs.org.

## References and Notes

(1) Faul, C. F. J. Antonietti, M. *Adv. Mater.* **2003**, *15*, 673−683.
(2) Binnemans, K. *Chem. Rev.* **2005**, *105*, 4148−4204.
(3) Zhou, S.; Chu, B. *Adv. Mater.* **2000**, *12*, 545−556.
(4) Zakrevskyy, Y.; Stumpe, J.; Faul, C. F. J. *Adv. Mater.* **2006**, *18*, 2133−2136.
(5) Franke, D.; Vos, M.; Antonietti, M.; Sommedijk, N. A. J. M.; Faul, C. F. J. *Chem. Mater.* **2006**, *18*, 1839−1847.
(6) Zakrevskyy, Y.; Faul, C. F. J.; Guan, Y.; Stumpe, J. *Adv. Funct. Mater.* **2004**, *14*, 835−841.
(7) Guan, Y.; Zakrevskyy, Y.; Stumpe, J.; Antoniettia, M.; Faul, C. F. J. *Chem. Commun.* **2003**, 894−895.
(8) Camerel, F.; Strauch, P.; Antonietti, M.; Faul, C. F. J. *Chem.—Eur. J.* **2003**, *9*, 3764−3771.
(9) Zhang, T.; Spitz, C.; Antonietti, M.; Faul, C. F. J. *Chem.—Eur. J.* **2005**, *11*, 1001−1009.
(10) Faul, C.F. J.; Antonietti, M. *Chem.—Eur. J.* **2002**, *8*, 2764−2768.
(11) Guan, Y.; Antonietti, M.; Faul, C. F. J. *Langmuir* **2002**, *18*, 5939−5945.
(12) Camerel, F.; Faul, C. F. J. *Chem. Commun.* **2003**, 1958−1959.
(13) General, S.; Antonietti, M. *Angew. Chem., Int. Ed.* **2002**, *41*, 2957−2960.
(14) Canilho, N.; Kasëmi, E.; Mezzenga, R.; Schlüter, A. D. *J. Am. Chem. Soc.* **2006**, *128*,13998−13999.
(15) Ozer, B. H.; Smarsly, B.; Antoniettia, M.; Faul, C. F. J. *Soft Matter* **2006**, *2*, 329−336.
(16) Thünemann, A. F.; Ruppelt, D.; Burger, C.; Müllen, K. *J. Mater. Chem.* **2000**, *10*, 1325−1329.
(17) Thünemann, A. F.; Ruppelt, D.; Ito, S.; Müllen, K. *J. Mater. Chem.* **1999**, *9*, 1055−1057.
(18) Zhou, S.; Shi, H.; Zhao, Y.; Jiang, S.; Lu, Y.; Cai, Y.; Wang, D.; Han, C. C.; X u, D. *Macromol. Rapid Commun.* **2005**, *26*, 226−231.
(19) Thünemann, A. F. *Langmuir* **2000**, *16*, 824−828.
(20) Gohy1, J.-F.; Antoun1, S.; Sobry, R.; den Bossche, G. V.; Jérôme, R. *Macromol. Chem. Phys.* **2000**, *201*, 31−41.
(21) Thünemann, A. F.; General, S. *Langmuir* **2000**, *16*, 9634−9638.
(22) Li, H.; Zhang, X.; Zhang, R.; Shen, J.; Zhao, B.; Xu, W. *Macromolecules* **1995**, *28*, 8178−8181.
(23) Antonietti, M.; Conrad, J.; Thünemann, A. *Macromolecules* **1994**, *27*, 6007−6011.
(24) O'Neill, M.; Kelly, S. M.; J. *Phys. D: Appl. Phys.* **2000**, *33*, 67−84.
(25) Alcalá, R.; Giménez, R.; Oriol, L.; Piñol, M.; Serrano, J. L.; Villacampa, B.; Viñuales, A. I. *Chem. Mater.* **2007**, *19*, 235−246.
(26) Stewart, D.; Imrie, C. T. *Polymer* **1996**, *37*, 3419−3425.
(27) He, X.; Zhang, H.; Yan, D.; Wang, X. *J. Polym. Sci., Part A: Polym. Chem.***2003**, 2854−2864.
(28) Acierno, D.; Amendola, E.; Bugatti, V.; Concilio, S.; Giorgini, L.; Iannelli, P.; Piotto, S. P. *Macromolecules* **2004**, *37*, 6418−6423.
(29) He, X.; Yan, D.; Mai, Y. J. *Eur. Polym. J.* **2004**, 1759−1765.
(30) Gibbons, W. M.; Shannon, P. J.; Sun, S. T.; Swetlin, B. J. *Nature (London)* **1991**, *351*, 49−50.
(31) Ramanujam, P. S.; Pedersen, M.; Hvilsted, S. *Appl. Phys. Lett.* **1999**, *74*, 3227−3229.
(32) Li, X.; Lu, X. M.; Lu, Q. H.; Yan, D.Y. *Macromolecules* **2007**, *40*, 3306−3312.
(33) Rochon, P.; Batalla, E.; Natansohn, A. *Appl. Phys. Lett.* **1995**, *66*, 136−138.
(34) Kim, D. Y.; Tripathy, S. K.; Li, L.; Kumar, J. *Appl. Phys. Lett.* **1995**, *66*, 1166−1168.
(35) Ubukata, T.; Seki, T.; Ichimura, K. *Adv. Mater.* **2000**, *12*, 1675−1678.
(36) Bai, S.; Zhao, Y. *Macromolecules* **2002**, *35*, 9657−9664.
(37) Bolle, M.; Lazare, S. *J. Appl. Phys.* **1993**, *73*, 3516−3524.
(38) Hiraoka, H.; Sendova, M. *Appl. Phys. Lett.* **1994**, *64*, 563−565.
(39) Csete, M.; Marti, O.; Bor, Zs. *Appl. Phys. A: Mater. Sci. Process.* **2001**, *73*, 521−526.
(40) Lu, Q. H.; Wang, Z. G.; Yin, J.; Zhu, Z. K.; Hiraoka, H. *Appl. Phys. Lett.* **2000**, *76*, 1237−1239.
(41) Lu, X. M.; Lu, Q. H.; Zhu, Z. K. *Liq. Cryst.* **2003**, *30*, 985−990.
(42) Lu, X. M.; Lu, Q. H.; Zhu, Z. K.; Yin, J. *Chem. Phys. Lett.* **2003**, *337*, 433−438.
(43) Lu, X. M.; Lu, Q. H.; Zhu, Z. K.; Yin, J.; Wang, Z. G. *Polymer* **2003**, *44*, 4501−4507.
(44) Zhang, D.; Liu, Y. X.; Wan, X. H.; Zhou, Q. F. *Macromolecules* **1999**, *32*, 5183−5185.
(45) Bazuin, C. G.; Boivin, J.; Tork, A.; Tremblay, H.; Bravo-Grimaldo, E. *Macromolecules* **2002**, *35*, 6893−6899.
(46) Tork, A.; Bazuin, C. G. *Macromolecules* **2001**, *34*, 7699−7706.
(47) Canilho, N.; Kasëmi, E.; Schlüter, A. D.; Mezzenga, R. *Macromolecules* **2007**, *40*, 2822−2830.
(48) Pan, X.; Wang, C.; Xu, H.; Wang, C.; Zhang, X. *Appl. Phys. B: Laser Opt.* **2007**, *86*, 693−697.
(49) Sipe, J. E.; Young, J. F.; Preston, J. S.; van Driel, H. M. *Phys. Rev. B* **1983**, *27*, 1141−1154.

MA070972S